Available online at www.sciencedirect.com
SCIENCE DIRECT
Polymer 46 (2005) 167–172
polymer
www.elsevier.com/locate/polymer

# Study on morphology and crystal growth of syndiotactic polystyrene solution-grown crystals by transmission electron and atomic force microscopy

Nobuyuki Suto, Atsuhiro Fujimori*, Toru Masuko

*Department of Polymer Science and Engineering, Faculty of Engineering, Yamagata University, Jonan 4-3-16, Yonezawa, Yamagata 992-8510, Japan*

Received 29 October 2003; received in revised form 9 October 2004; accepted 27 October 2004
Available online 23 November 2004

**Abstract**

The morphology of solution-grown crystals (SGCs) of syndiotactic polysthyrene (s-PS) has been investigated using transmission electron and atomic force microscopy (TEM and AFM). Well-defined s-PS SGCs were prepared from 0.005% (w/w) *n*-tetradecane/decahydronaphthalene solution 2:1 (v/v) by an isothermal crystallization method at 200 °C. Lattice constants for this crystal estimated by TEM with the diffraction mode are $a=0.90$ nm, $b=2.88$ nm. AFM images of the folded chains on the surface of s-PS SGC suggested their alignment parallel to the direction of the growth face of the truncated-lozenge shaped crystal. The angle between the growth faces obtained from s-PS SGCs was 130°. Since, the value of 130° correspond to the {230} angle, the primary growth face of s-PS SGC was assigned to the (230) plane.


*Keywords:* Syndiotactic polystyrene; Crystal growth direction; Approach to observe folded chains by atomic force microscopy

## 1. Introduction

For the last few decades, progress in polymer synthesis has enable to manufacture syndiotactic polystyrene (s-PS) with excellent stereo-regularity [1]. This polymer exhibits higher melting point (≥270 °C) and spherulitic growth rate than isotactic polystyrene (i-PS) by one order of magnitude [2]. Accordingly, s-PS has been utilized as high performance plastic.

This s-PS indicates a very complicated polymorphism that has attracted the attention of a number of researchers. Many investigators have conducted studies on s-PS, and classified several different crystalline forms using a number of techniques including X-ray [3–13] and electron [14–21] diffraction, FT-IR spectroscopy [22–31], solid state NMR [1,31–34] and conformational energy analyses [35]. Guerra et al. [6] proposed that the crystalline α and β forms contain chains in the trans planar conformation (TTTT), whereas the crystalline δ and γ forms contain chains in the helical conformation (TTGG) with *s*(2/1)2 symmetry. The δ form indicates a group of clathrate structures in which the polymer is incorporates various solvent molecules. Both the α and β forms can be divided into modifications with different degrees of structural order. The two limiting 'disordered modifications' (α′ and β′) and two limiting 'ordered modifications' (α″ and β″) have been described. Chatani et al. [11] investigated the exact crystal structure of the β form by X-ray analysis, describing that the β form has the orthorhombic unit cell ($P2_12_12_1$ or *Pbnm*, $a=0.88$ nm, $b=2.88$ nm, $c$ (chain axis)$=0.51$ nm).

Tsuji et al. [16] independently reported that solution-grown crystals (SGCs) of s-PS correspond to the β″-modification, grown from a dilute solution of *n*-tetradecane/decahydronaphthalene [T/D] mixture. In their works, the selected-area electron diffraction pattern from the single crystal indicated that the molecular-chains are perpendicular to the basal surface of the platelet. These findings enabled them to propose a structural model in which the disorder is due to stacking faults that occur when alternately stacking two types of 'motifs' (a bimolecular

* Corresponding author. Tel./fax: +81 238 26 3073.
*E-mail address:* fujimori@yz.yamagata-u.ac.jp (A. Fujimori).

0032-3861/$ - see front matter © 2004 Elsevier Ltd. All rights reserved.
doi:10.1016/j.polymer.2004.10.083

layer). The motifs are distinguished from each other by the rotational orientation of the planar zig-zag backbone chain around the chain axis. The stacking faults occur statistically, the alternate stack of two types of motifs extending parallel to the *bc*-plane of the SGC. (Note that the assignment of the *a*- and *b*-axes in their report is different from those determined by other researchers).

Tosaka et al. [17] indicated that the faulted plane is virtually a vertical section of the SGC, which was deduced from the dark-field images of the s-PS SGC observed using a transmission electron microscope. Furthermore, Hamada et al. [18] and Tosaka et al. [19] quantified the probability of the presence of the stacking faults as the ratio of the number of faulted planes to the total planes.

Another modification, the β′-form, was observed in the samples prepared by melt crystallization. Tosaka et al. [21, 22] reported that this structure involves the continuous stacking of the same type of motifs. Recently, Woo et al. [36–41] studied the relationship between polymorphisms and the multiple melting behavior of s-PS bulk.

As mentioned above, although there have been numerous structural and polymorphic studies on s-PS in recent years, there have been very few reports on the morphology of SGCs of s-PS in forms of the folded chain, because these SGCs tend to form multilayered crystals with severe overgrowth. In this study, the surface structures and other morphological features of s-PS SGC were investigated. The morphological characteristics of the crystal growth face of s-PS SGC were examined in detail by transmission electron and atomic force microscopy (TEM and AFM). Furthermore, direct observations of the folded chains of s-PS on the surface of SGC using contact mode of AFM measurements in the nanoscale was attempted. The images obtained are compared with the crystal structure and discussed with respect to the mechanism of chain folding.

## 2. Experimental

### 2.1. Materials

The s-PS pellet ($M_w = 375{,}000$, $M_w/M_n = 3.0$) was kindly supplied by Idemitsu Petrochemical Co., Ltd, Japan, and was used without further purification.

### 2.2. Preparation of SGCs

The specimen was prepared according to the procedure previously described [16]. A 2:1 (v/v) mixture of *n*-tetradecane: decahydronaphthalene [T/D] was utilized as the solvent for SGC preparation. This mixed solvent was first introduced by Keith et al. to prepare the SGC of i-PS [42]. A 0.005 wt% solution of s-PS was prepared by dissolving the pellet in the boiling solvent (234 °C). The solution was then cooled to a crystallization temperature of 200 °C and held for 2 h.

### 2.3. Electron microscopy

The precipitated SGC of s-PS thus obtained were carefully transferred onto a carbon-coated sheet mesh, followed by shadowing with an Au/Pd alloy at the angle of 27°. The specimen was examined using a Philips CM-300 electron microscope at an acceleration voltage of 200 kV.

### 2.4. Scanning probe microscopy

A scanning probe microscopy (Seiko Instruments, SPA300 with SPI-3800 probe station) was performed at 23 °C. A small amount of [T/D] solution with suspended SGC was dropped onto a cleaved mica surface and desiccated at 60 °C for several days. A pyramid-shaped $Si_3N_4$ tip was used the specimen surface in cyclic contact mode experiments with a spring contact force of 0.09 N $m^{-1}$. Scan rates of 0.5–1.0 Hz (applied force: 1.0 nN) were used for mesoscopic scale measurements, and scan rates of 16–32 Hz (applied force: −9.0 nN) were used for nanoscopic scale measurements.

When the molecular level observation was performed, the *x*–*y* scanner was calibrated by measuring the standard mica surface, which exhibites a repeating unit length of 0.52 nm in the in-plane direction. It is noted that the apparent surface image is not the real structure, since, the spacing between the folded chains is anticipated to be much smaller than the curvature of the $Si_3N_4$ tip, about 20 nm, and the hollow parts between protruding folds may not be correctly traced. Hence, the absolute value of the height information in the *z*-direction was regarded to be inappropriate to evaluate. However, the existence of dimples or protrusions maybe reliable, that is, the resolution in the *x*–*y* plane of contact mode AFM should be sufficient to estimate the detailed surface structures at a few nanometer scales. In order to avoid false recognition, no image processing was performed for the AFM images.

## 3. Results and discussion

### 3.1. Morphological observation of s-PS SGCs

Fig. 1 shows an electron micrograph of a s-PS SGC with well-defined shape obtained from a 0.005 wt% [T/D] solution at 200 °C. Although, most of the SGCs displayed severe overgrowth and formed multilayered crystals, a few well-defined, monolayered crystals were obtained under this condition. These SGCs were truncated-lozenge shaped crystals. The angle between growth faces was estimated to be about 130°, as indicated in this figure. Furthermore, multi-layered SGCs were formed due to the screw dislocation mechanism under the same conditions, as shown in Fig. 2. This angle between the two growth faces was also about 130°. The lateral size of the s-PS SGCs in this study was about 2–6 μm, and their lamellar thickness

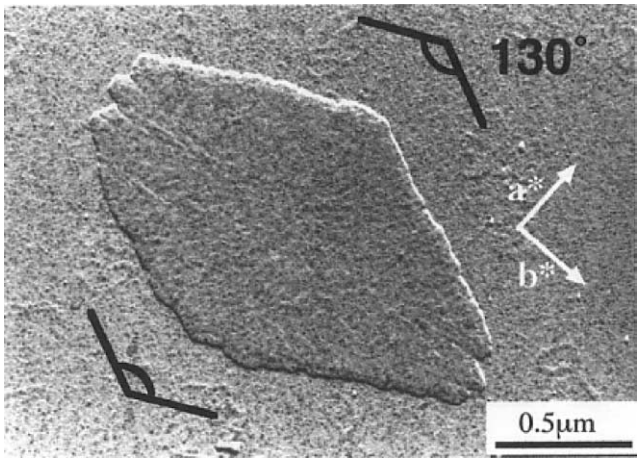


Fig. 1. Electron micrograph for SGC of s-PS. (insert) $a^*$ and $b^*$ arrows indicate the reciprocal lattice of this polymer.

was estimated from the shadow length to be approximately 10 nm.

### 3.2. Analysis of the electron diffraction pattern

The SGCs gave essentially the same electron diffraction (e. d.) patterns, as shown in Fig. 3(a). Fig. 3(b) shows the schematic illustration of the spot positions. The characteristic features of this e. d. pattern were described by Tsuji et al. [16] The $h00$ and $0k0$ reflections are absent for $h$ and $k$ odd; the extinction rule for reflections suggests that the two-dimensional space group is $p2gg$ in the $ab$-plane projection. Furthermore, the reflections corresponding to $h+k=2n$ ($n$: an integer) are spot-like, whereas others streak along the $b^*$-axis. It was suggested that the streaking of e. d. patterns attributed to the existence of 'stacking faults' in the s-PS SGC. Previously, the 'stacking faults' in the s-PS explained by De Rosa et al. [13] and Tsuji et al. [16] as follows: a pair of neighboring molecular layers extended parallel to the $ac$-plane (motif) are the basic structural units of s-PS crystals. The motifs are distinguished two type structures by the rotational orientation of the backbone chain. An alternating

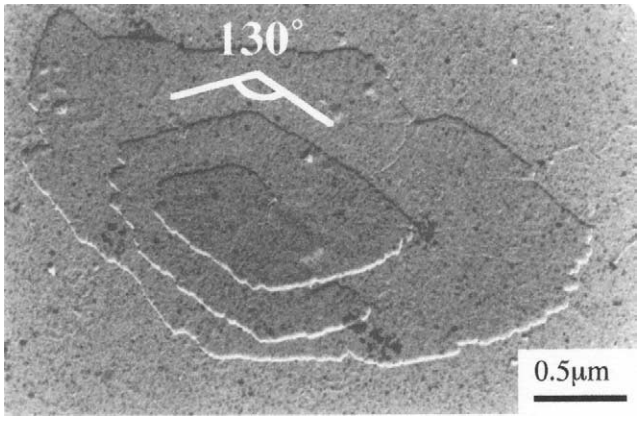


Fig. 2. Spiral dislocation growth for SGC of s-PS.

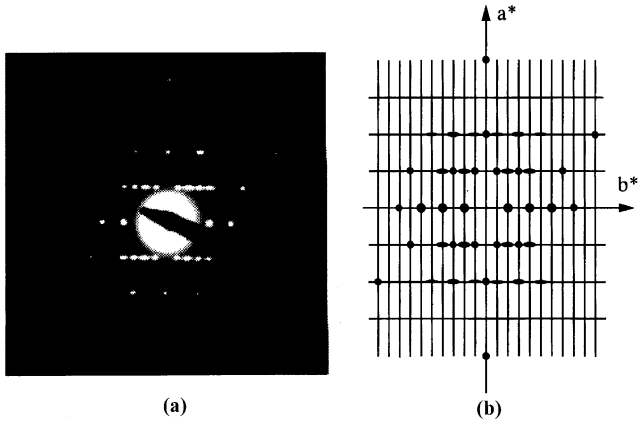


Fig. 3. (a) Selected-area electron diffraction pattern for the s-PS crystal. (b) Schematic illustration of the electron diffraction pattern in Fig. 3(a) ($a^*$ and $b^*$ indicate the reciprocal lattice of this polymer).

stack of these two motifs corresponds to the regular crystal lattice. A sequence having two motifs of the same type in succession is regarded as the 'stacking fault' in the s-PS. From the analysis of e. d. patterns in this study, reflections could be indexed as $hk0$ reflections on the basis of an orthorhombic unit cell with $a=0.90$ nm and $b=2.88$ nm. According to the Tsuji et al. [16], it was assigned the SGC exhibited these feature of the e. d. patterns to the $\beta''$-form crystal.

### 3.3. Surface morphology of s-PS SGC estimated by AFM

Fig. 4(a) shows the topographical image of a s-PS SGC by AFM. Images were captured while scanning without filters. In the AFM images, truncated-lozenge shaped crystals were observed. The SGC thickness values, about 9–10 nm, were in good agreement with those observed by TEM. Fig. 4(b) shows the enlarged image of the boxed area shown in Fig. 4(a). This figure also confirms the value of the angle between the growth faces to be 130°. In addition, a further enlarged image is shown in Fig. 4(c). In Fig. 4(c), the friction force microscope (FFM) image was adopted. The FFM image is able to more clearly indicate the anisotropic nature of the surface relative to topographic images, due to the direct detection of the changes in the friction force as the distortion and twisting of the probe during the scan in both the forward and reverse scan directions. Hundred nanometer wide streations running parallel to the $a$-axis were observed in this figure.

Fig. 5(a) and (b) shows the nanoscale AFM images of the folded chains on the surface of the truncated SGC [43]. For the AFM measurements, various images were recorded by 90° rotating the sample in a constant AFM scan direction (Fig. 5(c)), and compared with each other in order to judge whether the observed structures really exist or they are artifactual images. In this case, faster or slower scan rates resulted in unclear images in which it was difficult to confirm the lattice structure of the surface. It is important to

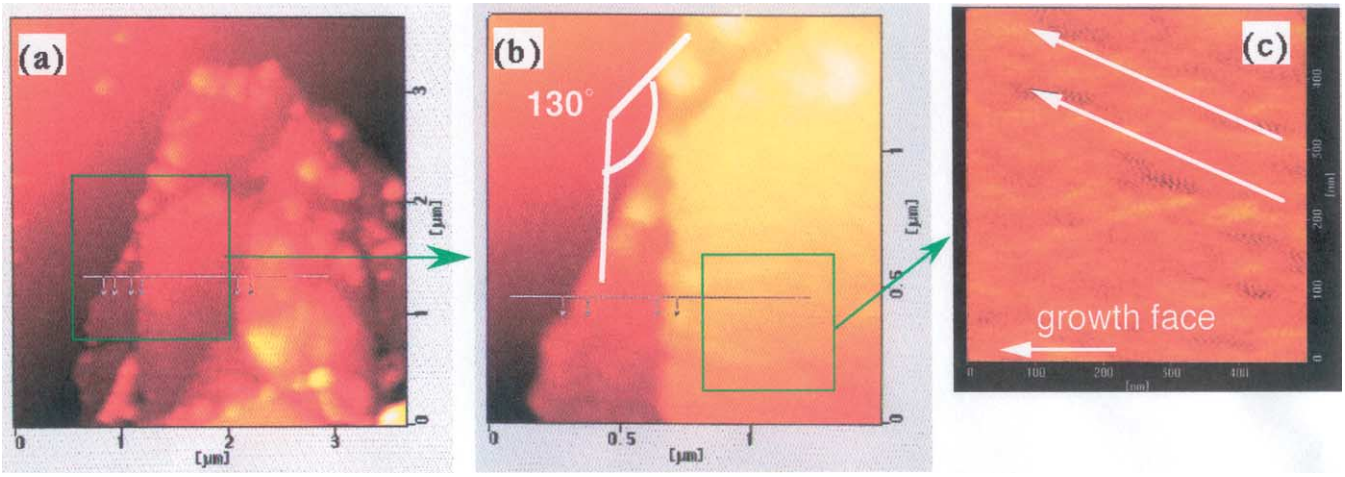


Fig. 4. Atomic force and friction force mesoscopic images for SGC of s-PS. (a) AFM image. (b) Enlarged image of part of (a). (c) Friction force image of part of (b).

note that these images were obtained using AFM tips with a relatively higher repulsive force, in order to reduce disordering or perturbing the arrangements of the folded chains. This image clearly reveals that folded s-PS chains are arranged in a more or less periodical structure. The white arrow in Fig. 5(d) indicates the direction perpendicular to the (230) growth face of the SGC. These AFM images were carried out for the direct observation of the folded chain of SGC for s-PS. In addition, the small image in the lower right-hand corner of Fig. 5(d) shows the Fourier transform (FT) pattern, which confirms that the surface pattern has a kind of regularity and symmetry. The FT pattern exhibits slight-distorted hexagonal spots related to the two-dimensionally ordered arrangement of folded chains, reflecting schematic illustration of two-dimensional lattice expressed by the white broken lines in Fig. 5(d). It is seemed that formation of the two-dimensional distorted hexagonal lattice in the outermost surface is slightly similar to the orthorhombic unit cell in the three-dimensional crystal. The cross sectional image along the dashed line in Fig. 5(d) indicates the periodic order aligned almost parallel to the (230) plane, which reflects the shape of folded s-PS chains. The spacing of the individual folded units lies in the range from 1.3 to 1.4 nm.

In general, the folded chains on the polymer crystal surfaces are considered to have a variety of chain lengths in which short and long chain loops coexist. Fig. 5(a) reveals that the fold chains are mainly composed of tight-chain loops. The nanoscale observations in contact AFM mode at ambient temperature are thought to be heavily influenced by local mode motions (ex. mainly internal rotation of about 10 monomer units) due to thermal vibrations. The s-PS exhibits relatively higher glass transition temperature and relaxation temperature of the local mode motion than other crystalline polymers, which prepared by solution growth (ex. polyethylene, polypropylene, etc.). Since, the existence of tightly packed loops having the rigid phenyl rings in the SGC can reduce the effect of thermal motion, it was suggested that approach to observe folded chains of s-PS SGC succeeded by a few nanometer scale AFM observation.

### 3.4. Determination of the direction of crystal growth

A schematic representation of the arrangement of the unit cell in the SGC is shown in Fig. 6. The growth face parallel to the (230) plane, and a 130° angle formed between (230) and (2$\bar{3}$0) planes are consistent with the obtuse angle formed by the two counter lines, as observed in Fig. 1. Although, Tuji et al. assigned (100) plane to growth face of s-PS single crystal [17], we regard (230) plane is more suitable for the growth face according to the obtuse 130° angle shown in Fig. 2.

According to the fractional coordinates of the atomic positions [11,13], the crystal structure model ($P2_12_12_1$) for the s-PS β″-form was constructed as shown in Fig. 7. The center of C–C bonds in the s-PS chains are aligned parallel to the (230) planes; chain folding is thought to occur along the {230} plane. The periodical arrangement of the folded chains would be spaced at about 1.57 nm. This value is expressed as the sum of two types of spacing 1.175 and 0.395 nm between the nearest neighboring unit cells, which depends on orientation of the phenyl units. The value of the sum, 1.57 nm, may correspond to the spacing between protrusions observed in the cross section diagrams of molecular resolution AFM images (Fig. 5(d)).

Solution grown crystals of s-PS possess specific characteristics, the ‘stacking faults’. The amount of stacking faults is thought to be dependent on the crystallization temperature. Hamada et al. reported that the amount of stacking faults decreased with an increase in the isothermal crystallization temperature [18]. The amount of stacking faults was thought to be low in this experiment. Therefore, the angle of the growth faces in this experiment were considered to be in agreement with the value for the crystal structure model of the β″-form. In addition, (230) faces were assumed to shift by $a/2$ in the course of the stacking

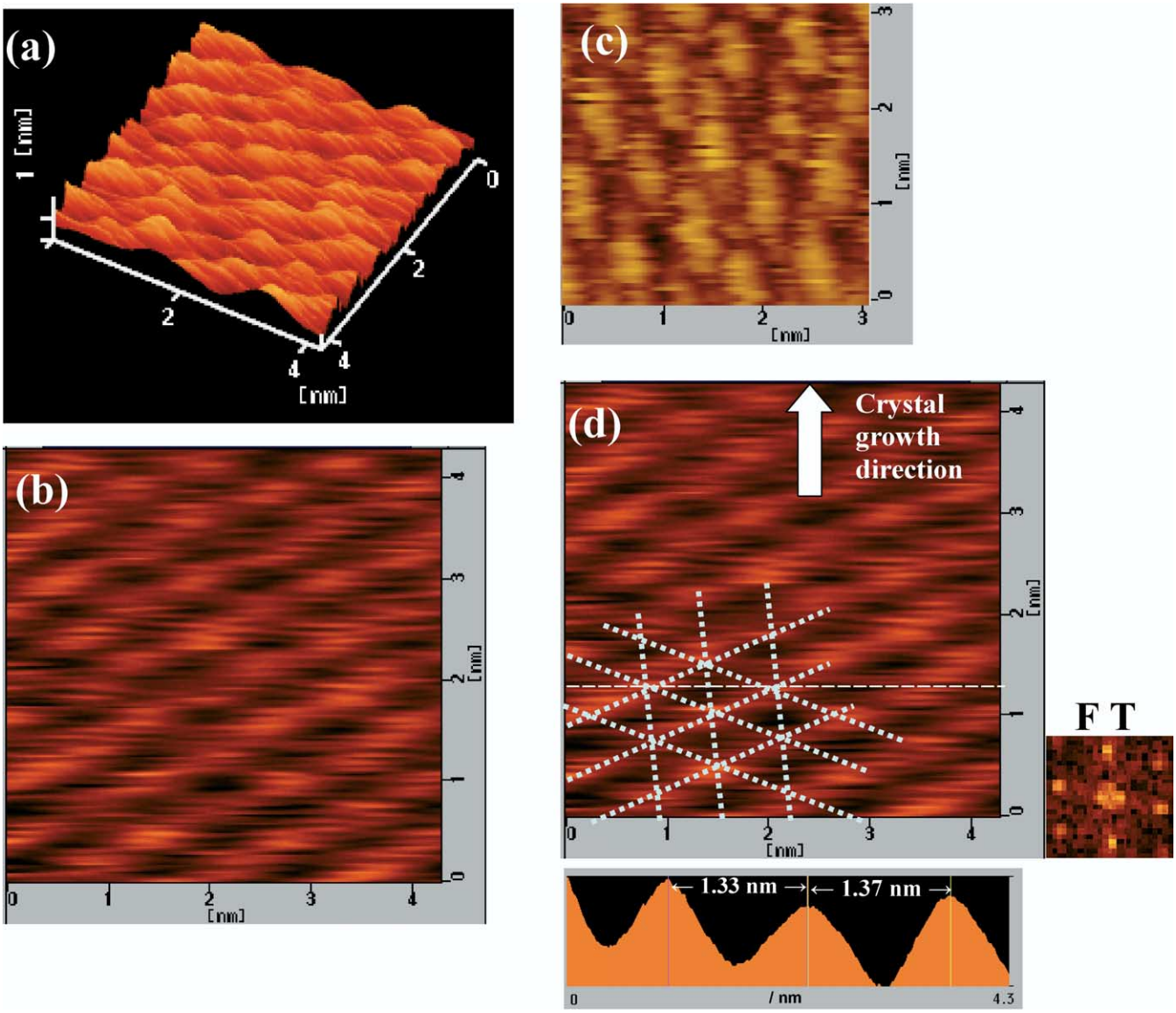


Fig. 5. Microscopic (nm scale) AFM images for SGC of s-PS. (a) Three-dimensional image. (b) Two-dimensional image. (c) Two-dimensional image obtained by different scanning direction at same scanning scale of Fig. 5(b). (d) AFM image with arrow indicated the crystal growth direction, cross section diagram and Fourier transform image.

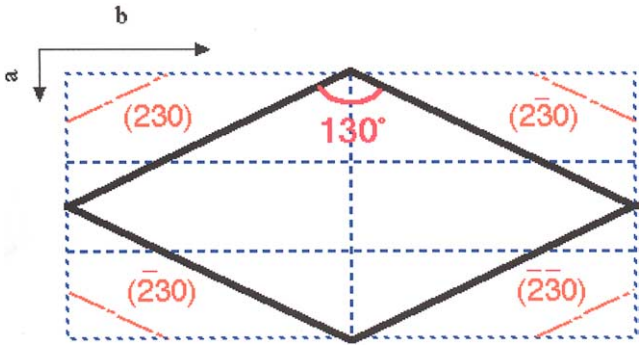


Fig. 6. Schematic illustration of crystal growth faces for SGC of s-PS.

faults in long-range order, because the (230) e. d. pattern exhibited streak like spots. This shift may be correlated with rough growth faces, which is observed in the macroscopic images. According to the overall interpretation of the results of this work, (230) faces were determined to be the primary growth faces of truncated-lozenge shaped s-PS SGCs.

## 4. Conclusions

Solution grown crystals of s-PS were prepared from 0.005% (w/w) *n*-tetradecane/decahydronaphthalene solution 2:1 (v/v) using an isothermal crystallization method. Their morphology and structural features were examined

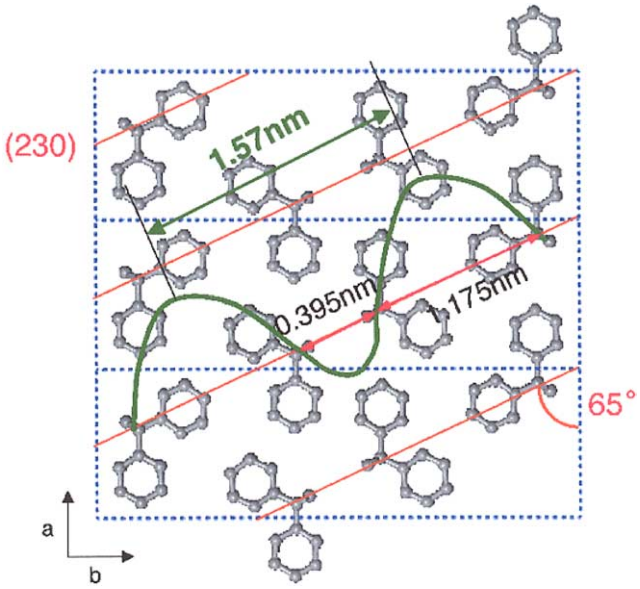


Fig. 7. Schematic representation of the crystal structure of the β″-form of s-PS.

using TEM and AFM observations. Well-defined s-PS SGCs were obtained at 200 °C. The SGC was assigned to be the β″-form according to characterization based on the e. d. pattern. TEM images showed the truncated-lozenge shaped crystal, with progressed spiral dislocation growth. The angle between two growth faces of the SGC was determined to be 130°, and accordingly the growth face of s-PS SGC was assigned to the (230) plane. In addition, the images of s-PS folded chains on the SGC surface was successfully obtained using AFM observation with nanoscale resolution. In those images, the periodical arrangements of the folded chains were observed with about 1.3–1.4 nm spacing, and they were aligned parallel to the direction of the SGC growth faces.

## References

[1] Ishihara N, Semiya T, Kuramoto M, Uoi M. Macromolecules 1986; 19:2464.
[2] Cimmino S, Pace ED, Martuscelli E, Silvestre C. Polymer 1991;32: 1080.
[3] Immirzi A, de Candia F, Iannelli P, Zambelli A. Makromol Chem Rapid Commun 1988;9:761.
[4] Vittoria V, Russo R, de Candia F. J Macromol Sci Phys 1989;B28: 419.
[5] Vittoria V, Russo R, de Candia F. Makromol Chem Macromol Symp 1990;39:317.
[6] Guerra G, Vitagliano VM, de Roza C, Petraccone V, Corradini P. Macromolecules 1990;23:1539.
[7] de Roza C, Guerra G, Petraccone V, Corradini P. Polym J 1991;23: 1435.
[8] Guerra G, de Rosa C, Vitagliano VM, Petraccone V, Corradini P. J Polym Sci: Part B, Polym Phys 1991;29:265.
[9] de Roza C, Rapacciuolo M, Guerra G, Petraccone V, Corradini P. Polymer 1992;33:1423.
[10] Auriemma F, Petraccone V, Dal Poggetto F, de Rosa C, Guerra G, Manfredi C, Corradini P. Macromolecules 1993;26:3772.
[11] Chatani Y, Shimane Y, Ijitsu T, Yukinari T. Polymer 1993;34:1625.
[12] Manfredi C, Guerra G, de Rosa C, Busico V, Corradini P. Macromolecules 1995;28:6508.
[13] de Rosa C. Macromolecules 1996;29:8460.
[14] Greis O, Xu Y, Asano T, Petermann J. Polymer 1989;30:590.
[15] Pradere P, Thomas EL. Macromolecules 1990;23:4954.
[16] Tsuji M, Okihara T, Tosaka M, Kawaguchi A, Katayama K. MSA Bull 1993;23:57.
[17] Tosaka M, Hamada N, Tsuji M, Kohjiya S, Ogawa T, Isoda S, Kobayashi T. Macromolecules 1997;30:4132.
[18] Hamada N, Tosaka M, Tsuji M, Kohjiya S, Katayama K. Macromolecules 1997;30:6888.
[19] Tosaka M, Hamada N, Tsuji M, Kohjiya S. Macromolecules 1997;30: 6592.
[20] Cartier L, Okihara T, Lotz B. Macromolecules 1998;31:3303.
[21] Tosaka M, Tsuji M, Cartier L, Lotz B, Kohjiya S, Ogawa T, Isoda S, Kobayashi T. Polymer 1998;39:5273.
[22] Tosaka M, Tsuji M, Kohjiya S, Cartier L, Lotz B. Macromolecules 1999;32:4905.
[23] Guerra G, Musto P, Karasz FE, MacKnight WJ. Makromol Chem 1990;191:2111.
[24] Filho AR, Vittoria V. Makromol Chem, Rapid Commun 1990;11:199.
[25] de Candia F, Filho AR, Vittoria V. Makromol Chem, Rapid Commun 1991;12:295.
[26] Vittoria V. Polym Commun 1990;31:263.
[27] Reynolds NM, Hsu SL. Macromolecules 1990;23:3463.
[28] Reynolds NM, Savage JD, Hsu SL. Macromolecules 1989;22:2867.
[29] Kobayashi M, Nakaoki T, Ishihara N. Macromolecules 1990;23:78.
[30] Reynolds NM, Stidham HD, Hsu SL. Macromolecules 1991;24:3662.
[31] Rastogi S, Gupta VD. J Macromol Sci Phys 1994;B33:129.
[32] Musto P, Tavone S, Guerra G, de Roza C. J Polym Sci: Part B, Polym Phys 1997;35:1055.
[33] Dais P, Nedea ME, Morin FG, Marchessault RH. Macromolecules 1990;23:3385.
[34] Capitani D, Segre AL, Grassi A, Sykora S. Macromolecules 1991;24: 623.
[35] Doherty DC, Hopfinger AJ. Macromolecules 1989;22:2472.
[36] Woo EM, Wu FS. Macromol Chem Phys 1998;199:2041.
[37] Sun YS, Woo EM. Macromolecules 1999;32:7836.
[38] Woo EM, Sun YS, Lee ML. Polymer 1999;40:4425.
[39] Rin RH, Woo EM. Polymer 2000;41:121.
[40] Sun YS, Woo EM. J Polym Sci, Part B: Polym Phys 2000;38:3210.
[41] Sun YS, Woo EM. Polymer 2001;42:2241.
[42] Keith HD, Vadimsky RG, Padden Jr FJ. J Polym Sci, A-2 1970;8: 1687.
[43] Suto N, Fujimori A, Masuko T. e-Polymers 2003;57:1.